JACS
JOURNAL OF THE AMERICAN CHEMICAL SOCIETY

COMMUNICATION

pubs.acs.org/JACS

$SrNbO_2N$ as a Water-Splitting Photoanode with a Wide Visible-Light Absorption Band

Kazuhiko Maeda,[†,§] Masanobu Higashi,[‡] Bhavin Siritanaratkul,[†] Ryu Abe,[‡] and Kazunari Domen*[,†]

[†]Department of Chemical System Engineering, The University of Tokyo, 7-3-1 Hongo, Bunkyo-ku, Tokyo 113-8656, Japan

[‡]Catalysis Research Center, Hokkaido University, North 21, West 10, Sapporo 001-0021, Japan

[§]Precursory Research for Embryonic Science and Technology (PRESTO), Japan Science and Technology Agency (JST), 4-1-8 Honcho, Kawaguchi, Saitama 332-0012, Japan

Supporting Information

ABSTRACT: Strontium niobium oxynitride ($SrNbO_2N$) particles were coated on fluorine-doped tin oxide (FTO) glass and examined as a photoelectrode for water splitting under visible light in a neutral aqueous solution (Na_2SO_4, pH ≈ 6). $SrNbO_2N$, which has a band gap of ca. 1.8 eV, acted as an n-type semiconductor and generated an anodic photocurrent assignable to water oxidation upon irradiation with visible-light photons with wavelengths of up to 700 nm, even without an externally applied potential. Under visible light (λ > 420 nm) with an applied potential of +1.0−1.55 V vs RHE, nearly stoichiometric H_2 and O_2 evolution was achieved using a $SrNbO_2N$/FTO electrode modified with colloidal iridium oxide (IrO_2) as a water oxidation promoter. This study presents the first example of photoelectrochemical water splitting involving an n-type semiconductor with a band gap smaller than 2.0 eV that does not require an externally applied potential.

Photoelectrochemical water splitting has attracted considerable attention as a potential means of converting solar energy into chemical energy in the form of H_2, which is a clean, renewable energy carrier. The research was inspired by a report from Fujishima and Honda in 1972, who demonstrated water splitting using a titanium dioxide single crystal as a photoanode and a platinum counter electrode with an external bias under UV irradiation.[1] Since then, many n-type metal oxide semiconductors, such as WO_3,[2] α-Fe_2O_3,[3] and $BiVO_4$,[4] have been employed as photoanodes in attempts to utilize visible-light photons, which are a major component of the solar spectrum. While these photoanodes exhibit excellent incident photon-to-electron conversion efficiencies (IPCEs) for water oxidation under certain conditions, they inherently require an externally applied potential. The tops of the valence bands of these metal oxides usually consist of O 2p orbitals, which are located at ca. +3 V or higher vs RHE. Therefore, if the bottom of the conduction band of a given metal oxide is more negative than the water reduction potential, the band gap inevitably is larger than 3 eV, rendering the material inactive in the visible-light region.[5] Certain (oxy)nitrides have recently been developed as alternatives to metal oxides for use as photoanode materials.[6−9] Since the valence band of (oxy)-nitrides is formed by N 2p orbitals or hybridized orbitals of N 2p and O 2p, the top of the valence band is negatively shifted, resulting in a smaller band gap for the (oxy)nitrides than for the corresponding metal oxides without affecting the potential of the conduction band.[10] Some of these materials can function as photoanodes for water oxidation, even without an externally applied potential.

A number of such photoanode materials have been developed to date. Some have achieved high IPCEs of several tens of percent with an applied bias smaller than the thermodynamically required potential for water electrolysis (1.23 V). In terms of available wavelength, photons with wavelengths up to 600 nm are available for photoelectrochemical water oxidation with α-Fe_2O_3,[3] $LaTiO_2N$,[7] and Ta_3N_5.[8] However, no photoanode with a band gap smaller than 2.0 eV (corresponding to a 600 nm absorption band) that can oxidize water without application of an external potential (except through the use of a tandem cell configuration[11]) has been reported to date. As the band gap of a given material is decreased, the driving forces for water oxidation and reduction should inevitably decrease, making water splitting more difficult.

Here we report a rare example of photoelectrochemical water oxidation using a porous $SrNbO_2N$ electrode. $SrNbO_2N$ is a perovskite-type oxynitride consisting of relatively earth-abundant metals that has a band gap of ca. 1.8 eV.[12] $SrNbO_2N$ powder also functions as a photocatalyst capable of oxidizing water to form O_2 under visible light in the presence of silver nitrate as an electron acceptor.[13] When particulate $SrNbO_2N$ is employed as a photoelectrode for visible-light-driven water splitting, it acts as an active photoanode to oxidize water, even without an externally applied potential. Nearly stoichiometric H_2 and O_2 evolution was observed during photoelectrolysis in a neutral electrolyte of Na_2SO_4 (pH ≈ 6) when a potential of +1.0−1.55 V vs RHE was applied.

$SrNbO_2N$ particles were prepared by our previously reported method.[13] As-prepared $SrNbO_2N$ was deposited on a fluorine-doped tin oxide (FTO) substrate by electrophoretic deposition[14] followed by calcination in air at 673 K for 0.5 h. A postnecking treatment to promote interparticle electron transfer[6,8b,9] was performed on the as-deposited $SrNbO_2N$ electrode using $NbCl_5$, and this was followed by heating under gaseous NH_3 at 753 K for 0.5 h. As a water oxidation promoter, colloidal IrO_2 prepared by hydrolysis of Na_2IrCl_6 at 353 K[15] was adsorbed on the

Received: April 13, 2011
Published: July 19, 2011

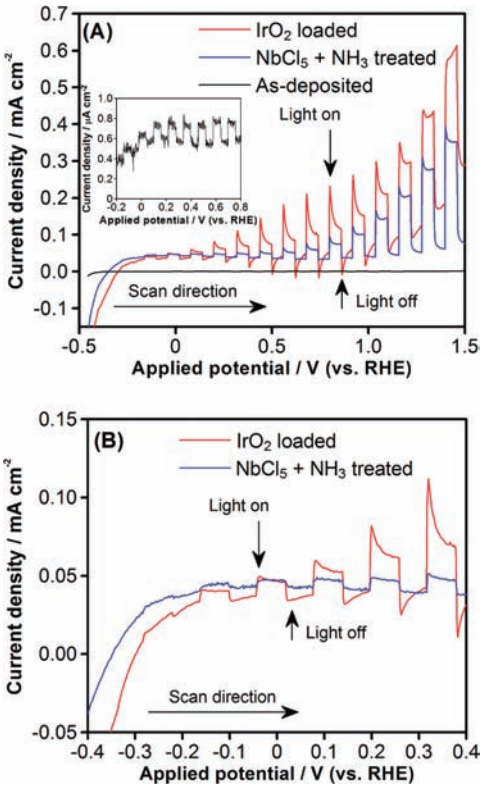

Figure 1. (A) Current−voltage curves in aqueous 0.1 M Na_2SO_4 solution (pH ≈ 6) under intermittent visible-light irradiation (λ > 420 nm) for modified $SrNbO_2N$ electrodes (2.5 cm^2). Scan rate: 20 mV s^{-1}. (B) Enlarged view of the lower-potential regions in (A).

NH_3-treated $SrNbO_2N$ electrode. The detailed preparation conditions are given in the Supporting Information (SI).

Figure 1A shows current−voltage curves for modified $SrNbO_2N$ electrodes under intermittent visible-light irradiation (λ > 420 nm). As-deposited $SrNbO_2N$ on an FTO substrate exhibited an anodic photoresponse (Figure 1A inset), indicating that $SrNbO_2N$ is an n-type semiconductor, although the photocurrent was very small in the potential range examined (less than 1 μA cm^{-2}). However, postnecking treatment of the as-deposited $SrNbO_2N$/FTO electrode with $NbCl_5$ followed by heating under NH_3 resulted in a drastic increase in the photocurrent as a result of the promotion of interparticle electron transfer.[6,8b,9] Scanning electron microscopy (SEM) observations revealed that the untreated $SrNbO_2N$ electrode exhibited a featureless morphology with a rough surface structure (Figure S2A in the SI), while postnecking treatment with $NbCl_5$ resulted in the interconnection of the $SrNbO_2N$ particles, slightly smoothing the surface structure (Figure S2B). The thickness of the coated particles was typically 2−3 μm as determined by SEM (Figure S2C). However, no noticeable change could be identified in the X-ray diffraction pattern of $SrNbO_2N$ before and after the postnecking treatment (Figure S3A). The color of the as-deposited $SrNbO_2N$ electrode turned darker after the postnecking treatment, suggesting that NbN and/or NbO_xN_y species having the valence states lower than Nb^{5+} were formed on the $SrNbO_2N$ particles. This was also supported by diffuse reflectance spectroscopy (DRS), which indicated that the absorption band at longer wavelengths was enhanced by the postnecking treatment (Figure S3B).

When colloidal IrO_2 was adsorbed on the postnecked electrode, the anodic photoresponse was further improved. In particular, the promotional effect was more pronounced in the lower-potential region than in the higher-potential region. IrO_2 is a well-known water oxidation catalyst,[15,16] and the present result clearly indicates that loading colloidal IrO_2 catalyst onto $SrNbO_2N$ promotes water oxidation. This idea was further supported by the results of the X-ray photoelectron spectroscopy (XPS) measurements, as will be shown later. The onset potential of the anodic photocurrent generated from the $IrO_2/SrNbO_2N$/FTO electrode ranged from approximately −0.3 to −0.1 V vs RHE.[17] This indicates that $SrNbO_2N$ functions as a water oxidation photoanode under visible light, even without an externally applied bias.[18] Furthermore, the onset potential was more negative than those of other n-type semiconductors such as α-Fe_2O_3,[3] Ta_3N_5,[7] and $LaTiO_2N$,[8] even though all of these have band gaps larger than that of $SrNbO_2N$. The dark current observed in the range +0.5−1.55 V can be attributed to the oxidation of NbN and/or NbO_xN_y species,[19] which were introduced by the postnecking treatment, and the water oxidation current (especially in the higher-potential range) derived from IrO_2 colloids that were probably directly attached to the FTO substrate. The $IrO_2/SrNbO_2N$/FTO electrode also generated an anodic photocurrent upon visible-light irradiation in a two-electrode configuration with a Pt wire cathode, although the performance was much lower than that in a three-electrode configuration (Figure S7). In addition, it was confirmed that the present electrode functions under simulated sunlight (Figure S8).

The ability of $SrNbO_2N$ to produce O_2 from H_2O using only light energy was also evidenced by the result of photocatalytic O_2 evolution from an aqueous $AgNO_3$ solution using $SrNbO_2N$ powder under visible-light irradiation. As shown in Figure S9A, it is clear that $SrNbO_2N$ is capable of producing O_2 under visible light (λ > 420 nm) even without any modification. Although $AgNO_3$ was used as an electron acceptor, no external energy other than visible light was supplied to the reaction system. It should be also noted that N_2 evolution, which has been sometimes observed in this reaction using (oxy)nitrides (e.g., $LaTiO_2N$, Ta_3N_5, and TaON),[10] could not be detected in the case of $SrNbO_2N$, indicating relatively good stability of this material among (oxy)nitrides. These results strongly suggest that the main contribution to the photocurrent generated at 0 V vs RHE is from water oxidation rather than the decomposition of $SrNbO_2N$, and they are also consistent with the results of cyclic voltammetry (CV) experiments using $SrNbO_2N$-based electrodes (Figure S6), in which no oxidation peak was observed. Moreover, when colloidal IrO_2 was loaded on $SrNbO_2N$ powder, the rate of O_2 evolution was enhanced by an order of magnitude, with no N_2 evolution (Figure S9B). This clearly demonstrates that IrO_2 on $SrNbO_2N$ promotes visible-light-driven water oxidation without promoting the decomposition of $SrNbO_2N$, which is in good qualitative agreement with the photoelectrochemical data at 0 V vs RHE (Figure 1B). The fact that the improvement in the photocurrent achieved by IrO_2 modification was more pronounced in the lower-potential region than in the higher-potential region also suggests that the photocurrent generated in the former contains a greater contribution from water oxidation than from decomposition of the electrode, because the photocurrent generated in the higher-potential region tended to contain a contribution from oxidative self-decomposition of the electrode, and that a upward band-bending

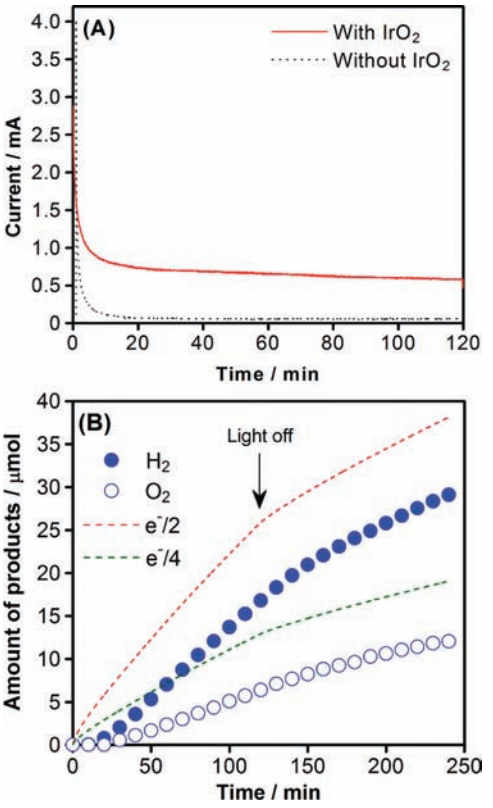

Figure 2. (A) Current−time curves in aqueous 0.5 M Na_2SO_4 solution (pH ≈ 6) for postnecked $SrNbO_2N$ electrodes (6 cm^2) with and without modification by colloidal IrO_2 at +1.55 V vs RHE under visible-light irradiation (λ > 420 nm). (B) Corresponding time courses of gas evolution in photoelectrochemical water splitting using an IrO_2-modified electrode.

at the interface between $SrNbO_2N$ and the electrolyte solution to drive water oxidation on $SrNbO_2N$ should become large. The same tendency has been observed for other photoanode materials, such as α-Fe_2O_3,[3c] TaON,[6b] Ta_3N_5,[7b] and $LaTiO_2N$.[8a]

Current−time curves recorded using postnecked $SrNbO_2N$/FTO electrodes with and without colloidal IrO_2 modification are shown in Figure 2A. During this experiment, an external bias of 1.55 V vs RHE was applied under steady-state visible-light irradiation (λ > 420 nm). The current generated from the electrode without IrO_2 decayed quickly during the initial stage of photoelectrolysis. XPS measurements, which typically analyze the surface of a solid material to a depth of several nanometers, showed that the nitrogen content obviously decreased from N/Nb = 0.52 to 0.12 upon photoelectrolysis (Table S1 and Figure S10), indicating the occurrence of photooxidative self-decomposition of the electrode. The IrO_2-modified electrode, however, exhibited relatively stable performance, although it did degrade slightly during the initial stage of the photoelectrolysis. These results strongly suggest that the adsorbed IrO_2 colloids on $SrNbO_2N$ suppress the oxidative self-decomposition of the material by improving the selectivity of photogenerated holes toward water oxidation, as has been reported for other (oxy)nitride-type photoanodes.[6b,7a,8b,9] The IrO_2-modified electrode was photoactive even after 120 min of photoelectrolysis, although the generated photocurrent in the higher-potential region was much lower than that observed for the fresh electrode (Figure S11). This is most likely due to the fact that the photooxidative decomposition was not completely suppressed even upon IrO_2 loading, as the nitrogen concentration decreased from N/Nb = 0.52 to 0.25.

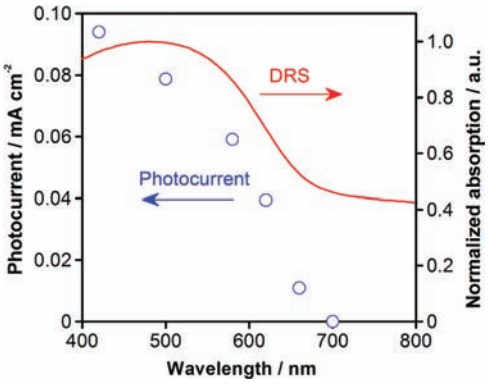

Figure 3. Dependence of the photocurrent generated by the IrO_2-modified $SrNbO_2N$ electrode (6 cm^2) at 0.95 V vs RHE in aqueous 0.1 M Na_2O_4 solution upon the cutoff wavelength of the incident light. The DRS spectrum of $SrNbO_2N$ is also shown. The spectral features of the light sources are displayed in Figure S14.

In any photoelectrochemical water splitting experiment, it is important to examine the evolution of H_2 and O_2, both of which should be generated by the water splitting reaction. As shown in Figure 2B, in the presence of an applied bias of +1.55 V vs RHE, nearly stoichiometric evolution of H_2 and O_2 was observed upon visible-light irradiation (λ > 420 nm), and the amounts increased with increasing time (from 0 to 120 min). The steady rates of H_2 and O_2 evolution (9.8 μmol h^{-1} for H_2 and 4.0 μmol h^{-1} for O_2) under irradiation were significantly higher than those recorded under dark conditions (5.3 and 2.4 μmol h^{-1}, respectively, from 120 to 240 min).[20,21] The dark current generated from the IrO_2-modified electrode (Figure S12) is attributed to oxidation of both water and the necked niobium species, as mentioned earlier. On the basis of the amounts of evolved H_2 and O_2, it was calculated that 47% of the visible-light current could be attributed to photoinduced water oxidation by IrO_2/$SrNbO_2N$. The amount of H_2 and O_2 detected were slightly less than half of what would be expected on the basis of the total electron flow, most likely because of the oxidation of NbN and/or NbO_xN_y species and formation of water from H_2 and O_2 on the Pt counter electrode.[6b] Nearly stoichiometric H_2 and O_2 evolution was detected in a similar experiment using an applied bias of ca. +1.0 V vs RHE, which is smaller than the thermodynamically required potential for water electrolysis (1.23 V). At that potential, the contribution from the dark current (Figure S6A) was relatively small, but the rates of H_2 and O_2 evolution were much smaller than those obtained at +1.55 V vs RHE (Figure S13). Below +1.0 V vs RHE, the water splitting rate was too slow to be detected.

Figure 3 shows the dependence of the photocurrent generated from a postnecked $SrNbO_2N$ electrode modified with colloidal IrO_2 at 0.95 V vs RHE on the cutoff wavelength of the incident light; the DRS spectrum of $SrNbO_2N$ is also shown. The photocurrent decreased with increasing cutoff wavelength, reaching almost zero at 700 nm, which corresponds to the absorption edge of $SrNbO_2N$. This result indicates that the photoelectrochemical water oxidation occurred through light absorption by $SrNbO_2N$ and that an absorption band at longer wavelengths, assignable to reduced Nb species (e.g., Nb^{4+}) that are defects in the material, did not contribute to the reaction.

The IPCE of the present IrO_2/$SrNbO_2N$/FTO electrode for water oxidation was calculated to be ca. 0.2% at 1.23 V vs RHE under irradiation with 400 nm monochromatic light.[22] The relatively low IPCE obtained here is at least in part due to the insufficient quality of the $SrNbO_2N$ powder used in this study. As can be seen in the DRS spectrum (Figure 3), the absorption band at longer wavelengths indicates the material contains a considerable number of defects, as mentioned above.

Nevertheless, it should be emphasized that no water-splitting photoanode that operates under irradiation at $\lambda > 600$ nm without an externally applied potential has been reported to date. The present result therefore demonstrates clear evidence that an n-type semiconductor with a band gap smaller than 2.0 eV can function as a photoanode for water splitting into H_2 and O_2, even without application of an external bias. It is expected that the performance of the $SrNbO_2N$ photoanode can be further improved by refining the $SrNbO_2N$ particle preparation method to reduce the density of defects in the material. Searching for more active water oxidation catalysts other than the present IrO_2 colloids would be another means of improving the electrode performance. Our current work is proceeding along these lines.

■ ASSOCIATED CONTENT

Supporting Information. Detailed experimental procedures and gas evolution data. This material is available free of charge via the Internet at http://pubs.acs.org.

■ AUTHOR INFORMATION

Corresponding Author
domen@chemsys.t.u-tokyo.ac.jp

■ ACKNOWLEDGMENT

This work was supported by the Research and Development in a New Interdisciplinary Field Based on Nanotechnology and Materials Science Program of the Ministry of Education, Culture, Sports, Science, and Technology (MEXT) of Japan and by The Kaiteki Institute, Inc. Acknowledgement is extended to the Cooperative Research Program of the Catalysis Research Center of Hokkaido University (Grant 10B1009) and a PRESTO/JST program.

■ REFERENCES

(1) Fujishima, A.; Honda, K. *Nature* **1972**, *238*, 37.

(2) (a) Hodes, G.; Cahen, D.; Manassen, J. *Nature* **1976**, *260*, 312. (b) Ulmann, M. S.; Augustynski, J. *J. Appl. Phys.* **1983**, *54*, 6061. (c) Santato, C.; Ulmann, M. S.; Augustynski, J. *J. Phys. Chem. B* **2001**, *105*, 936. (d) Amano, F.; Li, D.; Ohtani, B. *Chem. Commun.* **2010**, *46*, 2769. (e) Liu, R.; Lin, Y.; Chou, L.-Y.; Sheehan, S. W.; He, W.; Zhang, F.; Hou, H. J. M.; Wang, D. *Angew. Chem., Int. Ed.* **2011**, *50*, 499.

(3) (a) Hardee, K. L.; Bard, A. J. *J. Electrochem. Soc.* **1976**, *123*, 1024. (b) Kay, A.; Cesar, I.; Grätzel, M. *J. Am. Chem. Soc.* **2006**, *128*, 15714. (c) Tilley, S. D.; Cornuz, M.; Sivula, K.; Grätzel, M. *Angew. Chem., Int. Ed.* **2010**, *49*, 6405. (d) Hu, Y.-S.; Kleiman-Shwarsctein, A.; Stucky, G. D.; McFarland, E. W. *Chem. Commun.* **2009**, 2652. (e) Lin, Y.; Zhou, S.; Liu, X.; Sheehan, S.; Wang, D. *J. Am. Chem. Soc.* **2009**, *131*, 2772.

(4) (a) Sayama, K.; Nomura, A.; Zou, Z.; Abe, R.; Abe, Y.; Arakawa, H. *Chem. Commun.* **2003**, 2908. (b) Iwase, A.; Kudo, A. *J. Mater. Chem.* **2010**, *20*, 7536.

(5) Scaife, D. E. *Sol. Energy* **1980**, *25*, 41.

(6) (a) Abe, R.; Takata, T.; Sugihara, H.; Domen, K. *Chem. Lett.* **2005**, *34*, 1162. (b) Abe, R.; Higashi, M.; Domen, K. *J. Am. Chem. Soc.* **2010**, *132*, 11828.

(7) (a) Ishikawa, A.; Takata, T.; Kondo, J. N.; Hara, M.; Domen, K. *J. Phys. Chem. B* **2004**, *108*, 11049. (b) Yokoyama, D.; Hashiguchi, H.; Maeda, K.; Minegishi, T.; Takata, T.; Abe, R.; Kubota, J.; Domen, K. *Thin Solid Films* **2011**, *519*, 2087. (c) Feng, X.; LaTempa, J. T.; Basham, J. I.; Mor, G. K.; Varghese, O. K.; Grimes, C. A. *Nano Lett.* **2010**, *10*, 948.

(8) (a) Le Paven-Thivet, C.; Ishikawa, A.; Ziani, A.; Le Gendre, L.; Yoshida, M.; Kubota, J.; Tessier, F.; Domen, K. *J. Phys. Chem. C* **2009**, *113*, 6156. (b) Nishimura, N.; Raphael, B.; Maeda, K.; Le Gendre, L.; Abe, R.; Kubota, J.; Domen, K. *Thin Solid Films* **2010**, *518*, 5855.

(9) Hashiguchi, H.; Maeda, K.; Abe, R.; Ishikawa, A.; Kubota, J.; Domen, K. *Bull. Chem. Soc. Jpn.* **2009**, *82*, 401.

(10) Maeda, K.; Domen, K. *J. Phys. Chem. C* **2007**, *111*, 7851.

(11) Khaselev, O.; Turner, J. A. *Science* **1998**, *280*, 425.

(12) Kim, Y.; Woodward, P. M.; Baba-Kishi, K. Z.; Tai, C. W. *Chem. Mater.* **2004**, *16*, 1267.

(13) Siritanaratkul, B.; Maeda, K.; Hisatomi, T.; Domen, K. *ChemSusChem* **2011**, *4*, 74.

(14) Giersig, M.; Mulvaney, P. *Langmuir* **1993**, *9*, 3408.

(15) Harriman, A.; Pickering, I. J.; Thomas, J. M.; Christensen, P. A. *J. Chem. Soc., Faraday Trans. 1* **1988**, *84*, 2795.

(16) (a) Hoertz, P. G.; Kim, Y.-I.; Youngblood, W. J.; Mallouk, T. E. *J. Phys. Chem. B* **2007**, *111*, 6845. (b) Kuwabara, T.; Tomita, E.; Sakita, S.; Hasegawa, D.; Sone, K.; Yagi, M. *J. Phys. Chem. C* **2008**, *112*, 3774.

(17) The photocurrent onset potential of the IrO_2/$SrNbO_2N$/FTO electrode was shifted to slightly more positive potential (ca. −0.13 V) when polarization was made from positive to negative potential, with a reduction in the photocurrent (Figure S4).

(18) Additional evidence to support the idea that $SrNbO_2N$ photoanode works even without application of an external bias is the fact that $SrNbO_2N$ powder modified with Pt nanoparticles as water reduction promoters functions as a photocatalyst for H_2 evolution from an aqueous methanol solution under >300 nm irradiation (Figure S5) without any energy input other than light energy. It should be noted that a semiconductor must have the bottom of the conduction band above the water reduction potential in order for the semiconductor to achieve photocatalytic H_2 evolution from water.

(19) CV of the IrO_2-modified postnecked $SrNbO_2N$/FTO electrode in the dark indicated that the anodic dark current began to show up at +0.5 V vs RHE and increased gradually with anodic polarization to ca. +1.2 V and then sharply from +1.2 V (Figure S6). The CV behavior was almost reversible except for the first scan (Figure S6A). In view of both the overpotential of IrO_2 for water oxidation (typically as low as 0.25 V) and the fact that the unmodified $SrNbO_2N$/FTO electrode did not show any anodic dark current in the +0.5−1.55 V potential range (Figure S6B), the dark current observed in the +0.5−1.55 V range for the IrO_2-modified postnecked $SrNbO_2N$/FTO electrode can be attributed to the NbN and/or NbO_xN_y species introduced by the postnecking treatment (Figure S3B).

(20) The rates of H_2 and O_2 evolution were a little persistent just after light-off and then remained at a constant level. We believe this is not a poor light response of the electrode but rather a time lag in detection between current and gas evolution. In our photoelectrolysis system, evolved gases are detected by a micro-GC after they escape from the liquid-electrolyte phase into the gas phase (Figure S1).

(21) It was also noted that the amount of H_2 and O_2 produced by visible-light-induced water splitting exceeded 12 μmol (the difference between the amounts of evolved gases for the former 120 min and the latter 120 min), which is greater than the amount of the deposited niobium compounds (9.6 μmol) on FTO ($SrNbO_2N$, 6.6 μmol; NbO_xN_y and NbN, 3.0 μmol). This means that the photoelectrolysis of water occurs catalytically and is not merely due to self-oxidative decomposition of the $SrNbO_2N$ material itself.

(22) The current−voltage curve recorded in the IPCE measurement is shown in Figure S15, with spectral data for the light source.